Journal of Nuclear Materials 386–388 (2009) 557–560

Contents lists available at ScienceDirect

Journal of Nuclear Materials

journal homepage: www.elsevier.com/locate/jnucmat

TEM study of internal oxidation in an ODS-Eurofer alloy

M. Klimenkov *, R. Lindau, A. Möslang

Institute for Materials Research I, Forschungszentrum Karlsruhe GmbH, Hermann-von-Helmholtz-Platz 1, 76344 Eggenstein-Leopoldshafen, Germany

A B S T R A C T

Analytical TEM investigations of samples from an oxide dispersion-strengthened Eurofer batch show the formation of new type of precipitates of Fe–Cr–V–O composition and a size of 40–250 nm. Structural HRTEM analysis reveals that the precipitates consist of $(Mn,Fe)(Cr,V)_2O_4$ manganese chromium oxide of spinel structure. In some cases, the inclusions order along lines that can reach more than ten micrometers in length. Such lines of large particles might have a negative influence on the mechanical properties of the steel, as was observed. It is assumed that they form by internal oxidation during hot isostatic pressing due to the high oxygen content of the mechanically alloyed powder.

1. Introduction

Eurofer ODS (oxide dispersion-strengthened) steels presently are considered the main structural material candidates for advanced breeding blankets in fusion reactors plants, which is mainly due to the higher swelling resistance and low activation properties [1,2]. Recently developed reduced-activation ferritic-martensitic (RAFM) ODS steels on the basis of the European RAFM reference steel Eurofer 97 showed good tensile and creep properties, acceptable ductility, but poor impact behaviour. By selecting a specific production route for ODS-Eurofer steel of the second generation, which included rolling and appropriate thermal treatments, the DBTT was shifted from values between +60 and +100 °C for hipped ODS-Eurofer of the first generation to values between −40 and −80 °C [2,3]. The main goal of this development is to improve the creep resistance at high temperatures and, consequently, to increase the operating temperature in future fusion power reactors up to 650 °C.

Based on this experience, a 50 kg batch was produced by PLANSEE GmbH in different product forms: plates of 6 and 16 mm thickness, extruded rods of 12.5 and 20 mm in diameter. While the tensile properties of this so-called EU ODS-Eurofer batch are comparable or slightly better than those of the precursor alloy, the impact behaviour is worse (Fig. 1).

A TEM study was performed with the goal to find the reasons of this deterioration on the nanostructural level. The investigations show the presence of 30–300 nm large globular precipitates of a new type, which appear independently the thermal treatment applied. Application of high-resolution TEM (HRTEM) and analytical methods shows that these particles consist of an oxide phase. This result is rather unusual, because the presence of oxide precipitates inside ferritic alloys has never been reported in the scientific literature. Large Al oxide inclusions formed by an internal oxidation process were found in Al-containing ODS steels, such as PM-2000 [4]. In this paper, it will be reported about the comprehensive characterisation of the oxide precipitates in martensitic steels.

2. Experimental

The nominal chemical composition of the EU ODS-Eurofer batch investigated is 0.08C–9.3Cr–1.1W–0.35Mn–0.2V–0.08Ta + 0.3 wt% Y_2O_3. The samples of the 6 mm thick plate were austenitised between 980 and 1100 °C for 30 min and tempered at 750 °C for 2 h. Specimens for TEM characterisation were ground to ~130 μm thickness. From these discs, TEM samples of 3 mm diameter were punched and electro-polished in a TENUPOL device using 20% H_2SO_4 + 80% CH_3OH as electrolyte. The samples were additionally cleaned for a few minutes with an Ar ion beam at a low angle using a Precise Ion Polishing System made by Gatan Ltd.

The investigations were performed using a FEI Tecnai 20 F (200 kV, field emission gun) microscope equipped with a high-angle annular dark field (HAADF) detector for the scanning TEM. The electron energy loss spectroscopy (EELS) experiments were performed in the scanning TEM (STEM) regime. For EELS measurements, an energy resolution of 1.1 eV and dispersions of 0.1 eV/channel for one-edge spectra and 0.3 eV/channel for multi-edge spectra were employed. The electron beam used for imaging and analysis has a probe size of 1.0–1.2 nm. The EDX spectra were recorded using an EDAX Si/Li detector with an ultra-thin window. The quantitative EDX experiments focussed on the precipitates which were located on or near the specimen edge in order to avoid the influence of the matrix.

* Corresponding author.
E-mail address: michael.klimenkov@imf.fzk.de (M. Klimenkov).

0022-3115/$ - see front matter © 2009 Elsevier B.V. All rights reserved.
doi:10.1016/j.jnucmat.2008.12.176

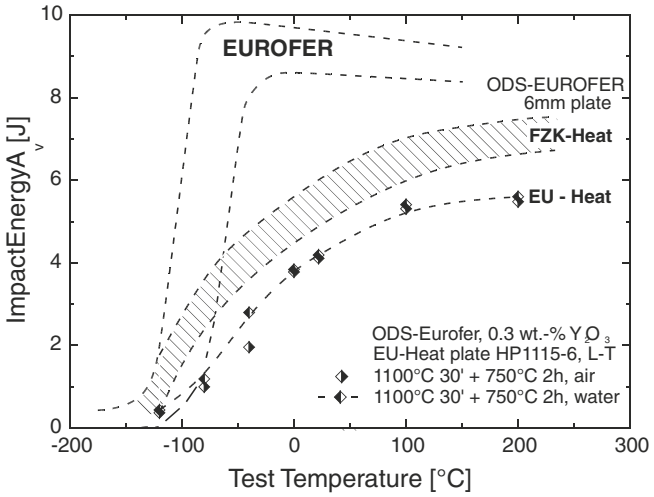

Fig. 1. Test temperature dependence of the total absorbed energy of ODS-Eurofer (FZK-Heat, EU-Heat) compared to RAFM steel Eurofer 97.

3. Results and discussion

STEM investigations using the HAADF detector show the presence of well visible precipitates with a darker contrast (Fig. 2). The precipitates have a round shape and their size varies from 30mn to 300 nm. According to statistical evaluations, their spatial density amounts to $(3 \pm 2) \times 10^{13}$ cm^{-3}. In most cases, the precipitates are statistically embedded in the matrix. However, areas in which they are ordered along the lines have also been observed (Fig. 2). These lines often extend to a length of more than 10 μm – the entire TEM transparent area on the specimen edge. Apparently, these lines are not coincident with the previous austenitic grains (Fig. 2). Fig. 1 shows the impact energy of this EU batch in comparison to the former FZK ODS-Eurofer heat and Eurofer base steel. The results clearly exhibit a higher ductile-to-brittle transition temperature (DBTT) and lower upper shelf energy (USE) compared to the precursory FZK ODS-Eurofer heat, independently of the heat treatment applied. It is assumed that the occurrence of the above-mentioned aligned precipitates is the reason of the deterioration of the impact properties.

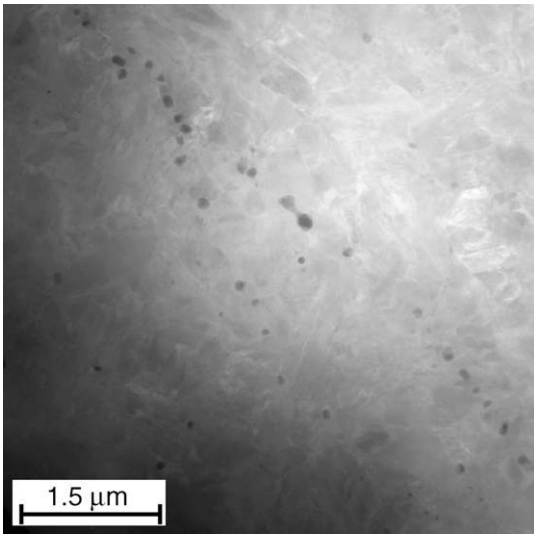

Fig. 2. HAADF image of an area with ordered precipitates.

Analytical investigations of the precipitates were performed using EDX and EELS methods. A typical EDX spectrum obtained from such an precipitate shows the presence of V, Cr, Mn, and Fe inside (Fig. 3(a)). The results of the quantitative evaluation of the spectrum are presented in Table 1. The precipitates were also investigated using EELS analysis (Fig. 3(b)). The background in the spectrum was corrected using power law. The spectrum clearly shows that additionally to V, Cr, and Mn detected by EDX, this precipitate also contains oxygen. In contrast to the EDX analysis, the EELS measurements clearly show the absence of Fe inside the precipitates. It is well known that the EELS method more reliably reveals the presence or lack of Fe inside a precipitate, because the lines in the EDX spectra might be influenced by several scattering effects which may contribute to the error of 3–4%. The EELS investigations have also shown that N or C are not present in the precipitate. Both analytical methods clearly demonstrate that the type of precipitate observed is V–Mn–Cr oxide. EDX mapping of 25 μm^2 areas confirms that all visible precipitates have the same composition. In this way, these precipitates may be distinguished clearly

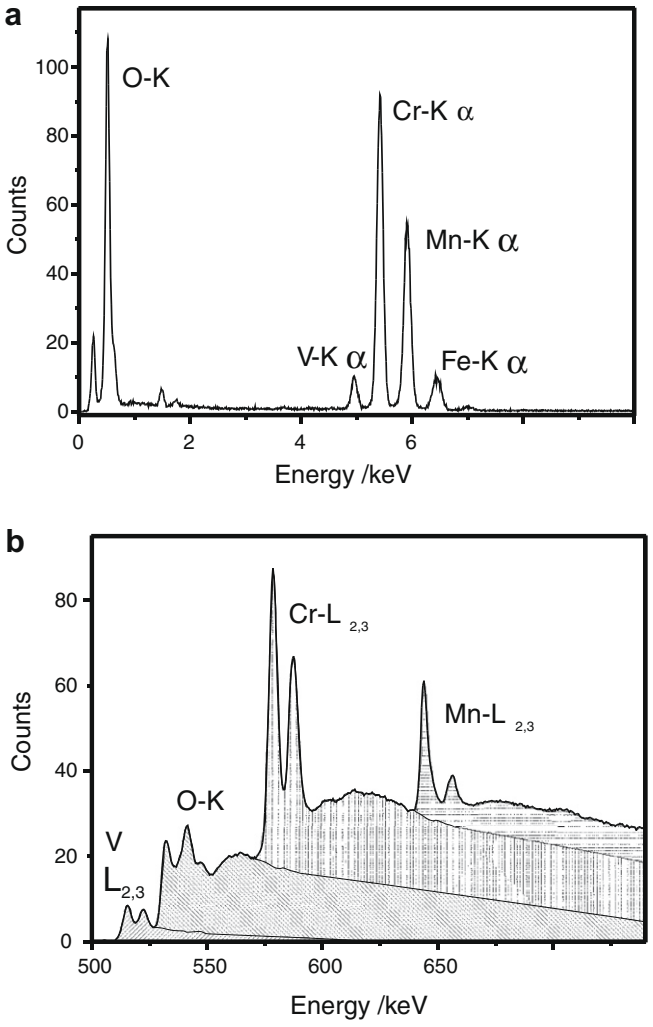

Fig. 3. The EDX (a) and EEL spectrum (b) of a precipitate.

Table 1
Chemical composition of the inclusion measured using the EDX method.

Element	Al	V	Cr	Mn	Fe
Weight/%	2.5	6.5	54	31	3

from carbide precipitates which appear in the samples after thermal treatments.

Phase identification of the oxide precipitates was performed using HRTEM. The image of a precipitate and its fast Fourier transformation (FFT) image are shown in Fig. 4. The two imaged atomic planes have 0.25 nm interplanar distance with an angle of 85° between them. This pattern was compared with several simulated diffraction patterns of known V—Mn—Cr oxides. It corresponds to the [521] orientation of a spinel structure with a lattice constant of 0.845 nm. According to theoretical calculations, the atomic planes of {3 1 1} type in this structure have a distance of d_{311} = 0.255 nm with an angle of 84.6° between them. Taking into account the measured chemical composition, the oxide precipitates may be suggested to consist of manganese chromium oxide of (Mn,Fe)(Cr,V)$_2$O$_4$ composition (patterns 31–630, 35–550, Ref. [5]). The measured (Mn, Fe)/(Cr, V) ratio of 1/2 (Table 1) is in a better correlation for (Mn, Fe) (Cr, V)$_2$O$_4$ spinel phase than for the other manganese chromium oxide phases with the same crystalline structure (patterns: 33–892, 44–909, 75–1614, and 71–982).

The spatially resolved analytical investigations reveal that the discussed oxide precipitates are not single-phased in most cases. Fig. 5 shows that the oxide inclusion has two smaller (Y,O)-rich particles which are located on precipitate/matrix interface. The precipitate was scanned with an electron beam in the STEM regime in order to simultaneously acquire the EELS and EDX spectra at each point. Such investigations allow for the imaging of the spatial distribution of both 3-d metals and light (C,N,O) elements. The HAADF image of the precipitate is presented in Fig. 5(a). Fig. 5(b)–(e) display the spatial distributions of Fe, Cr, Mn, and Y, respectively. As can be seen, the Fe concentration is reduced to zero in the particle (Fig. 5(b)). The Cr and Mn elemental maps clearly show increasing concentrations inside the precipitate (Figs. 5(c) and (d)). At the lower edge of the particle, two 40 nm areas depleted of Fe, Cr, V, and Mn are clearly visible. These areas exhibit a bright contrast in the Y and O map (Figs. 5(e) and (g)). The particles consist of a Y_2O_3 phase – the typical compound of ODS particles. As expected, the V-$L_{2,3}$ signal increases in the particle. Additionally, the V-map clearly shows the formation of a V-rich layer around the precipitate. Its thickness was measured to vary from 7 nm on the left side of the to 3 nm on the right side. The layer does not completely surround the precipitate (Fig. 5f). It is missing in several precipitate/matrix interface regions. The O–K elemental map (Fig. 5(g)) shows that the spatial distribution of oxygen also correlates with the precipitate, the two Y_2O_3 particles as well as the V-rich layer. Direct identification of the phase of the layer is not possible using HRTEM or diffraction methods due to its small thickness.

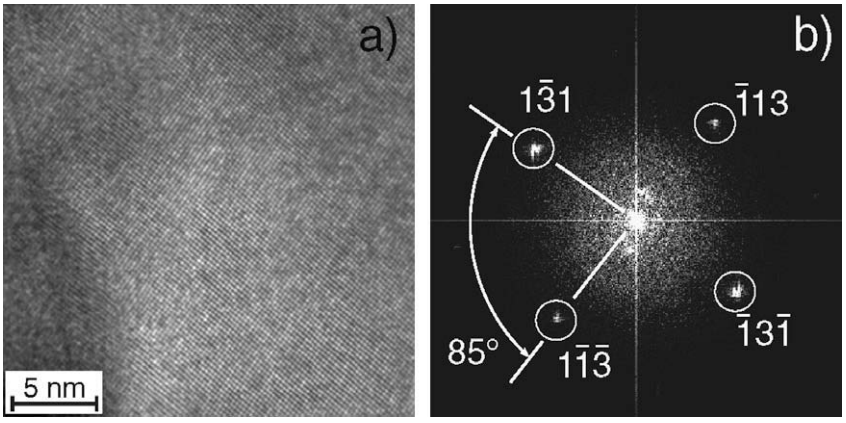

Fig. 4. HRTEM image of a precipitate (a) and corresponding fast Fourier transformation image.

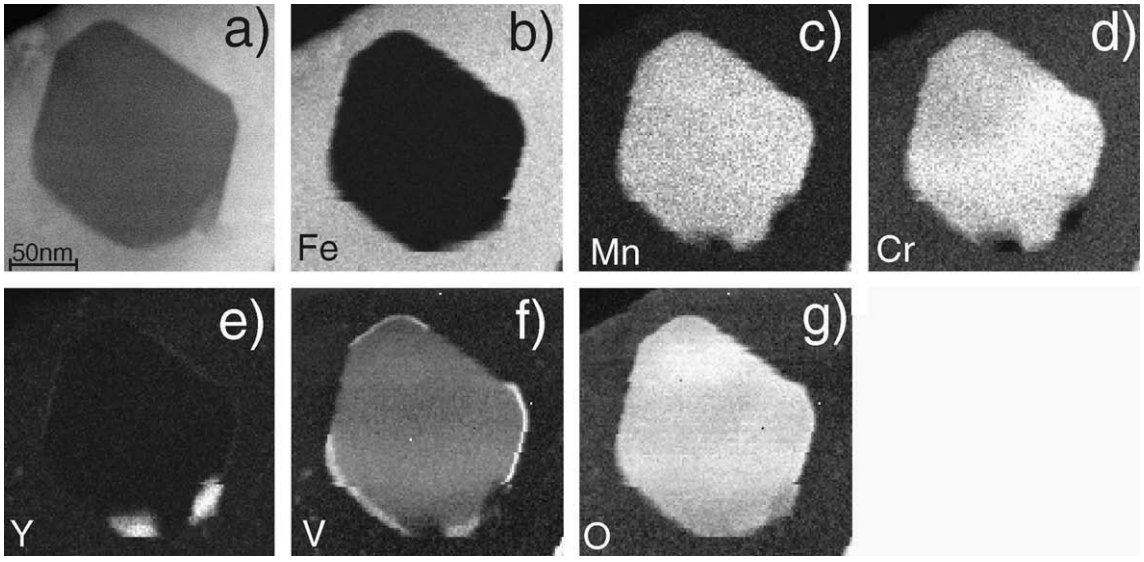

Fig. 5. HAADF image of a precipitate (a) and Fe, Mn, Cr, Y, V, and O elemental maps in figures (b)–(g), respectively.

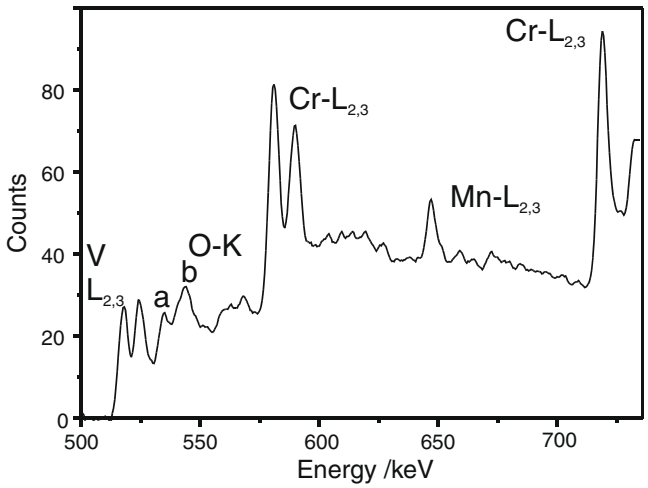

Fig. 6. The EELS spectrum of the V-rich area which surrounds oxide precipitates.

Hints concerning the V oxide phase may be obtained by an energy loss near edge structure analysis of O–K edges. This structure may be used as a "fingerprint" for phase identification. The EELS spectrum shown in Fig. 6 was obtained from V-rich thin layer (Fig. 5). The spectrum exhibits changes in the O–K fine structure compared to the EELS spectrum obtained from the Mn (Cr, V)$_2$O$_4$ precipitate with spinel structure (Fig. 3(b)). The O–K fine structure in both oxide parts clearly reveals the presence of two features at 531 and 545 eV, which are marked by an "a" and "b" in Fig. 6. The intensity ratio I_a/I_b of these two features decreases in the V-rich layer from approximately 7/8 for spinel oxide to the value of 5/8. The position of the peak "b" remains the same as for the manganese chromium oxide, whereas peak "a" shifts towards higher energy at 2 eV. Both features are also present in the ELNES of 5 different V oxide polymorphs. Comparison of the position and intensity of these two features with reference materials suggests that the thin V-rich shell consists of the V_2O_3 phase [6].

4. Conclusion

TEM analysis of Eurofer ODS steel has shown the presence of unexpected precipitates in the ferritic-martensitic steel. Application of combined EDX/EELS analysis shows that the precipitates detected are oxides. Additional structural HRTEM analysis confirms the formation of an (Mn,Fe)(Cr,V)$_2$O$_4$ phase. The oxide precipitates may originate from the internal oxidation of the powder, which takes place during fabrication. Oxidation during mechanical alloying leads to an oversaturation of the matrix with oxygen and the formation of oxide precipitates during HIPing. The presence of these precipitates in the microstructure of the EU ODS-Eurofer batch clearly differs from earlier produced heats [3]. The impact behaviour of the material may be affected negatively by the alignment of these precipitates.

References

[1] R. Lindau, A. Möslang, M. Schirra, P. Schlossmacher, M. Klimenkov, J. Nucl. Mater. 306–310 (2002) 769–772.
[2] R. Lindau, M. Klimiankou, A. Möslang, M. Rieth, B. Schedler, J. Schröder, A. Schwaiger, in: Proceedings 16th International Plansee Seminar 2005 Reutte Austria, vol. 1, 2005, pp. 545–557.
[3] M. Klimiankou, R. Lindau, A. Möslang, J. Nucl. Mater. 367–370 (2007) 173–178.
[4] M. Klimiankou, R. Lindau, A. Moeslang, J. Schröder, Powder Metall. 48 (2005) 277–287.
[5] ASTM Standard, Am. Soc. Test. Mat., Philadelphia, PA, 1988.
[6] C. Hebert, M. Willinger, D.S. Su, P. Pongratz, P. Schattschneider, R. Schlogl, Eur. Phys. J. B 28 (2002) 407–414.